Superconducting vortices generated via spin-orbit coupling at superconductor/ferromagnet interfaces

L. A. B. Olde Olthof,[1,*] X. Montiel,[1,†] J. W. A. Robinson,[1,‡] and A. I. Buzdin[2,3,1,§]

[1]*Department of Materials Science and Metallurgy, University of Cambridge, CB3 0FS Cambridge, United Kingdom*
[2]*University Bordeaux, LOMA UMR-CNRS 5798, F-33405 Talence Cedex, France*
[3]*Sechenov First Moscow State Medical University, Moscow 119991, Russia*

Spin-orbit coupling (SOC) plays an important role at superconductor/ferromagnet interfaces. By using the generalized London and Ginzburg-Landau theories, we demonstrate that SOC induces spontaneous vortices in zero applied magnetic field in an *s*-wave superconductor placed below a ferromagnetic metal with intrinsic or interfacial SOC. Even for small SOC strength, the interaction between SOC and vortices is attractive, pinning vortices along the edges of the ferromagnet with the SOC reinforcing the superconducting state. This Rapid Communication also highlights experimental schemes to investigate these phenomena, which provide a platform for Abrikosov vortex memory.

In an *s*-wave superconductor (S), charge flows in the absence of dissipation but since the Cooper pairs consist of electrons with antiparallel spins (singlet pairs), the current does not carry a net spin. The opposite occurs in a ferromagnetic (F) metal in which an internal exchange field h_{ex} creates a mismatch in the density of states of electrons with up and down spins, meaning that dissipative currents flow with a net spin polarization [1]. At a S/F interface, h_{ex} interacts within S over the superconducting coherence length which for Nb is $\xi = 30\text{–}40$ nm [2], whilst in F the interaction is shorter with $\xi_F = 1\text{–}3$ nm in Co [3–5], Fe [4,6], and Ni [3–5] due to h_{ex} dephasing the singlet pairs. Hence there is a F-thickness-dependent modulation of the critical temperature T_c [7] in S/F bilayers and critical current I_c in S/F/S Josephson junctions [8–10]. In F_1/S/F_2 [11–15] or F_1/F_2/S [16–19] spin valves, the total exchange field acting on the S layer is controllable via magnetization alignment of the F layers, which creates a dependence of T_c on magnetic configuration or I_c in S/F_1/F_2/S Josephson junctions [20–22]. A nonparallel alignment of magnetizations between F layers converts singlet pairs to spin-aligned triplet pairs [23–25] in which triplet supercurrents carry a net spin [26–32]. These phenomena form the basis of applications in superconducting spintronics [33].

Spin-orbit coupling (SOC) is also present at S/F interfaces due to broken inversion symmetry [23,24,34–37] and is enhanced by introducing a material with strong SOC between the S and F layers. Spin is not conserved in the presence of SOC, since the SOC rotates spin towards the direction of

magnetization and hence, at S/F interface can result in spin-aligned triplet pairs [38,39], e.g., in a recent ferromagnetic resonance experiment on Pt/Nb/Py [40–42], spin-pumping efficiency was enhanced below T_c indicating a spin-triplet channel in Nb over ξ, which forms due to SOC in Pt in combination with h_{ex} from Py.

Interfacial SOC adds a Rashba contribution $H_R = (\alpha_R/\hbar)(\hat{n} \times \vec{p}) \cdot \vec{\sigma}$ to the energy, where α_R is the Rashba SOC strength, $\vec{\sigma}$ is the electron spin, $\vec{p}$ is the orientation of the momentum, and $\hat{n}$ is the unit vector along the broken inversion symmetry axis. Magnetic order spin polarizes electrons, meaning that momentum along $\vec{\sigma} \times \hat{n}$ is energetically favorable [43] and induces spontaneous currents. This is predicted near S/F interfaces within the London penetration depth from the interface [43], around magnetic islands on a thin S [44,45], in a closed S loop partially covered by a ferromagnetic insulator [46] and in a thin S in contact with a Néel skyrmion [47]. In this Rapid Communication we investigate the interaction of SOC and vortices in S/F structures at temperatures T at and below T_c. By applying realistic material parameters, we derive a criterion for spontaneous vortex generation in zero applied magnetic field due to SOC, and demonstrate that SOC strongly affects transport in S/F junctions.

We model a type-II S of thickness d_S (with $d_S < \xi$) that is partially covered by a thin-film metallic F of thickness d_F, as shown in Figs. 1(a) and 1(b). We use the general Ginzburg-Landau (GL) approach to describe the system where the density of the free energy $F = \int f(\vec{r}) d^3\vec{r}$ is

$$
\begin{aligned}
f = {} & a|\psi|^2 + \frac{b}{2}|\psi|^4 + \frac{1}{4m}|\hat{D}\psi|^2 \\
& + \frac{h^2}{8\pi} + \frac{\vec{\alpha}}{4m} \cdot [\psi^* \hat{D}\psi + \psi(\hat{D}\psi)^*],
\end{aligned} \tag{1}
$$

where $a = a_0(T - T_c)/T_c$ and b are the standard GL coefficients, ψ is the superconducting order parameter,

---

[*]labo2@cam.ac.uk
[†]xm252@cam.ac.uk
[‡]jjr33@cam.ac.uk
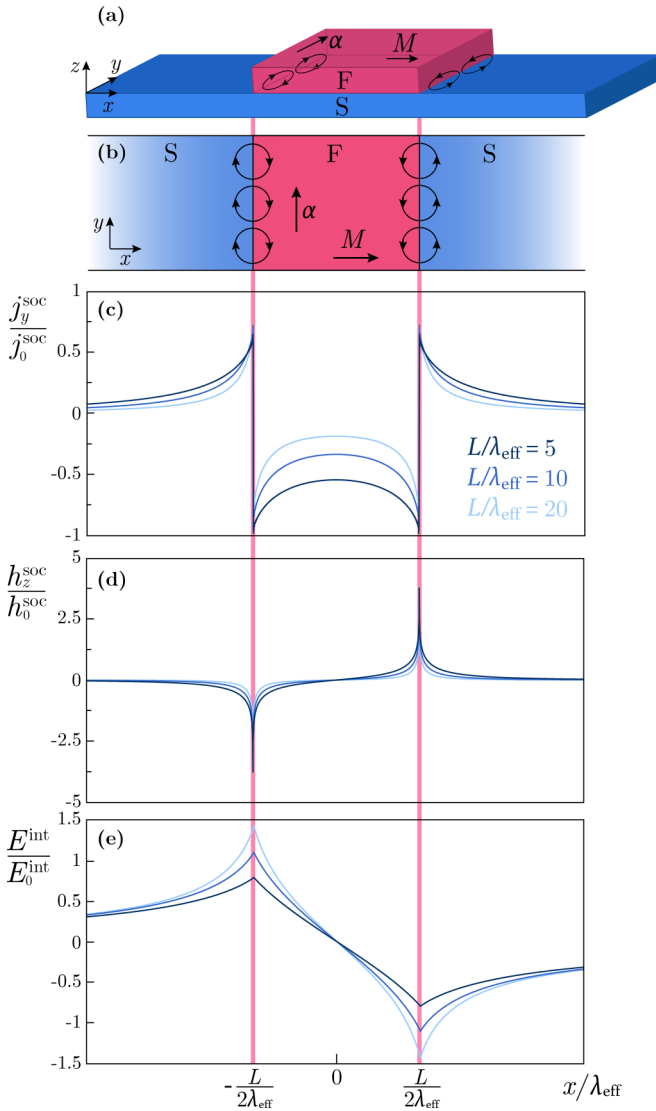[§]alexandre.bouzdine@u-bordeaux.fr

FIG. 1. A ferromagnetic strip on a superconductor at $T \ll T_c$. (a) A perspective and (b) top view of the S/F heterostructure with magnetization $\vec{M}$ and SOC $\vec{\alpha}$. Vortices and antivortices are represented by circular currents at the F edges. (c) The current $j_y^{\text{SOC}}/j_0^{\text{SOC}}$ and (d) the magnetic field $h_z^{\text{SOC}}/h_0^{\text{SOC}}$ due to SOC. (e) The interaction energy between the vortices and SOC $E^{\text{int}}/E_0^{\text{int}}$.

$\hat{D} = -i\vec{\nabla} + 2e\vec{A}$ is the gauge-invariant momentum operator with $\hbar = c = 1$, and $\vec{h}$ is the magnetic induction. The magnetization of F is in-plane along x resulting in SOC along y. SOC in the F is described by $\vec{\alpha} = \alpha \Theta(x - L/2)\Theta(L/2 - x)\hat{y}$, where $\Theta(x)$ is the Heaviside step function and the SOC strength α is [48]

$$\alpha \simeq \frac{v_R}{v_F} \frac{c}{d_S} \frac{h_{\text{ex}}}{T_c \xi}, \qquad (2)$$

where $\phi_0/2\pi = 1/2e$ is the flux quantum, c is the atomic lattice parameter, $v_R = \alpha_R/\hbar$ the Rashba velocity, and v_F the Fermi velocity. The gradient over the order parameter appears only in the presence of SOC and a ferromagnetic exchange field [49,50]. The SOC α varies over ξ. We consider the F/S heterostructure in the London framework, which describes

field variations over distances of $\lambda \gg \xi$. On this scale, α is a step function.

For $T \ll T_c$, superconductivity is well developed, such that the GL order parameter is $\psi = |\psi|e^{i\varphi}$, where $|\psi|$ is constant and φ is the phase of the superconducting order parameter [51]. Following Ref. [52], we introduce the vorticity

$$\vec{\Phi} = \phi_0 \frac{\hat{n} \times (\vec{r} - \vec{r}_0)}{(r - r_0)^2} \qquad (3)$$

to describe the phase singularity related to a vortex at $\vec{r} = \vec{r}_0$. Assuming $d_S \ll \lambda$, superconductivity along z can be taken constant, such that its integral yields a factor d_S. We define the effective penetration depth as $\lambda_{\text{eff}} = \lambda^2/d_S$ [52]. The free energy is then

$$F = F_0 + \frac{1}{8\pi\lambda_{\text{eff}}} \int \left[(\vec{\Phi} - \vec{A})^2 + \frac{\vec{\alpha}}{e} \cdot (\vec{\Phi} - \vec{A}) \right] d^2\vec{r}$$
$$+ \int \frac{h^2}{8\pi} d^3\vec{r}, \qquad (4)$$

where F_0 is the free energy in the normal state, above T_c.

The current density in the plane $z = 0$ is given by $\vec{j} = -\partial f/\partial\vec{A} \, \delta(z)$. From the Maxwell-Ampere equation $4\pi\vec{j} = \vec{\nabla} \times \vec{h} = -\Delta\vec{A}$, we obtain [51]

$$-\Delta\vec{A} = \frac{1}{\lambda_{\text{eff}}}\left(\vec{\Phi} - \vec{A} + \frac{\vec{\alpha}\phi_0}{2\pi} \right)\delta(z), \qquad (5)$$

which in Fourier space, has solution $\vec{A}_q$ [the two-dimensional Fourier transform of $\vec{A}(z = 0)$] [51,53]:

$$\vec{A}_q = \frac{\vec{\Phi}_q + \vec{\alpha}_q\phi_0/2\pi}{1 + 2|\vec{q}|\lambda_{\text{eff}}}. \qquad (6)$$

$\vec{A}_q$ consists of two contributions $\vec{\Phi}_q$ and $\vec{\alpha}_q$, which are terms that describe the two-dimensional Fourier transforms of the vortices $\vec{\Phi}$ and SOC $\vec{\alpha}$, respectively [51]. Following [52], we use $\vec{A}_q$ to derive several physical quantities. The current density $\vec{j} = -\partial f/\partial\vec{A}\,\delta(z)$ consists of two terms, i.e., $\vec{j} = \vec{j}^{\text{vor}} + \vec{j}^{\text{SOC}}$. The vortex contribution $\vec{j}^{\text{vor}}$ is given in Ref. [52]. The current generated due to SOC is

$$\vec{j}^{\text{SOC}}(x) = j_0^{\text{SOC}}\hat{y} \int_0^\infty \frac{\sin\left(\frac{p(\frac{L}{2}-x)}{\lambda_{\text{eff}}}\right) + \sin\left(\frac{p(\frac{L}{2}+x)}{\lambda_{\text{eff}}}\right)}{1 + 2p} dp \qquad (7)$$

with $j_0^{\text{SOC}} = \frac{\alpha\phi_0}{4\pi^3\lambda_{\text{eff}}}$ and $p = q_x\lambda_{\text{eff}}$. The local magnetic field at the surface of the superconductor is obtained by transforming the Maxwell equation $\vec{h} = \vec{\nabla} \times \vec{A}$ into Fourier space. The magnetic field consists of two contributions $\vec{h} = \vec{h}^{\text{vor}} + \vec{h}^{\text{SOC}}$, of which the first is known [52] and the SOC contribution is

$$\vec{h}^{\text{SOC}}(x) = h_0^{\text{SOC}}\hat{z} \int_0^\infty \frac{\cos\left(\frac{p(\frac{L}{2}-x)}{\lambda_{\text{eff}}}\right) - \cos\left(\frac{p(\frac{L}{2}+x)}{\lambda_{\text{eff}}}\right)}{1 + 2p} dp \qquad (8)$$

with $h_0^{\text{SOC}} = \frac{\alpha\phi_0}{2\pi^2\lambda_{\text{eff}}}$. The interaction between the vortices and SOC is described by the cross terms ($\sim\vec{\alpha}_q \cdot \vec{\Phi}_q^* + \vec{\alpha}_q^* \cdot \vec{\Phi}_q$) in the total free energy (4). We obtain

$$E^{\text{int}}(x) = -E_0^{\text{int}} \int_0^\infty \frac{\sin\left(\frac{pL}{2\lambda_{\text{eff}}}\right) \sin\left(\frac{px}{\lambda_{\text{eff}}}\right)}{p(1 + 2p)} dp \qquad (9)$$

with $E_0^{\text{int}} = \frac{\alpha\phi_0^2}{2\pi^3}$.

The current density (7), magnetic field (8), and interaction energy (9) are plotted in Figs. 1(c)–1(e). These quantities are proportional to the SOC strength α and depend on the F strip's width L. Since the SOC is an edge effect located inside the F, the current exhibits a discontinuity at the F strip's edges. The SOC causes local spikes in the magnetic field at the edges, which are positive and negative, corresponding to the in-plane magnetization direction [here directed along the vector $\hat{x}$; see Fig. 1(b)] [54]. The interaction energy attracts vortices towards its minimum at $-L/2$ and repels vortices from its maximum at $L/2$ (an antivortex).

The behavior of $\vec{j}^{\text{SOC}}(x)$ and $E^{\text{int}}(x)$ follows the same trend in Ref. [55], even though the physical origin in [55] is electromagnetic, and not SOC. The interaction between the vortex and edge of the F in [55] is generated by stray fields, which is proportional to the magnetization M and d_F. The SOC mechanism here dominates if $\alpha\phi_0/2\pi^2 > 2Md_F$. Taking into account that the lower critical field of the S is $h_{c1} = (\phi_0/4\pi\lambda^2)\ln(\lambda/\xi)$, this condition can be written as $\alpha > B(0)\pi d_F/h_{c1}\lambda^2$, where $B(0) = 4\pi M$ is the magnetic induction in the F. For $B(0) \sim h_{c1}$ and $d_F \sim d_S \sim \xi$, this condition is fulfilled for typical values of α needed for vortex generation [see Eq. (13) below]. The sign of the current generated by the SOC mechanism may be opposite to the current due to the electromagnetic interaction, since it depends on the sign of the exchange integral determining h_{ex}.

We use Eq. (9) to derive the criterion for spontaneous nucleation of vortices without applied magnetic field (see [51]). In the presence of SOC, h_{c1} is modified to

$$h_{c1} = \frac{4\pi}{\phi_0}(E^{\text{vor}} + E^{\text{int}}), \quad (10)$$

where E^{vor} is the energy of vortices [52]

$$E^{\text{vor}} = \left(\frac{\phi_0}{4\pi}\right)^2 \frac{1}{\lambda_{\text{eff}}} \ln\left(\frac{\lambda_{\text{eff}}}{\xi}\right). \quad (11)$$

The term E^{int} describes the interaction between vortices and SOC and writes in the limit $L \gg \lambda_{\text{eff}}$ [51]

$$E^{\text{int}} \simeq -\frac{\alpha\phi_0^2}{4\pi^3} \ln\left(\frac{L}{\lambda_{\text{eff}}}\right). \quad (12)$$

This interaction is negative implying that h_{c1} decreases in the presence of SOC. The spontaneous generation of vortices occurs when h_{c1} becomes negative, i.e., when the positive energy of the vortices is balanced by the negative interaction. The SOC strength required for the formation of vortices is then

$$\alpha > \frac{\pi}{4\lambda_{\text{eff}}} \frac{\ln(\lambda_{\text{eff}}/\xi)}{\ln(L/\lambda_{\text{eff}})}. \quad (13)$$

Equation (13) shows that an increase in h_{ex} or L or a reduction in d_S favors vortex creation. Typical ratios in Eq. (2) are $v_R/v_F \sim 0.1$ [56,57] and $ch_{\text{ex}}/d_S T_c \sim 0.1$ [46], giving $\alpha \simeq 0.01/\xi$. By assuming $\xi/\lambda_{\text{eff}} \sim 10^{-3}$ and $\xi \ll L$, (13) is satisfied and spontaneous vortex-antivortex pairs form with the antivortex (vortex) chain under the left (right) edge of the F in Figs. 1(a) and 1(b). A calculation and discussion of the linear density of the vortices is given in [51].

So far, we have considered the case where the superconductivity is well developed. For $T \lesssim T_c$, the superconductivity
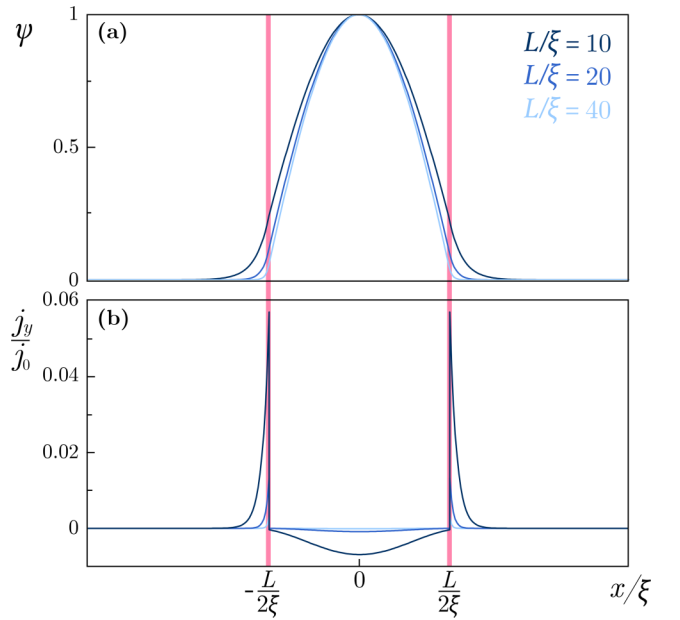

FIG. 2. A ferromagnetic strip on a superconducting film at $T = T_c$. Spatial dependence of (a) the normalized wave function $\psi(x)$ and (b) the current density $j_y(x)$ for different (labeled) lengths L/ξ.

is weak and we have to calculate the order parameter space dependency explicitly [51]. Minimizing f [Eq. (1)], the GL equation in the absence of a magnetic field is

$$a\psi + b|\psi|^2\psi - \frac{1}{4m}\left(\frac{\partial^2\psi}{\partial x^2} + \frac{\partial^2\psi}{\partial y^2}\right) - \frac{i\alpha}{2m}\frac{\partial\psi}{\partial y} = 0. \quad (14)$$

At T_c, the order parameter magnitude vanishes ($|\psi|^2 \to 0$) and the GL equation can be linearized [51]. Solving Eq. (14) for ψ and calculating the current $\vec{j}$, we find [51]

$$\vec{j}(x) = \begin{cases} j_0|\psi(x)|^2\hat{y} & \text{for } |x| > L/2, \\ -\varepsilon j_0|\psi(x)|^2\hat{y} & \text{for } |x| < L/2, \end{cases} \quad (15)$$

where $j_0 = e\alpha/m$ and ε is a small difference between the modulation vector and α, which is found self-consistently [51].

The wave function $\psi(x)$ and current density $j_y(x)$ from Eq. (15) are shown in Fig. 2. The current density $j_y(x)$ exhibits large peaks at the edges and a small suppression inside the F. Comparing Fig. 2(b) to 1(c), the current goes up near the edge at $T = T_c$, which results from suppression of the order parameter.

In general, when $T \lesssim T_c$, the order parameter is $\psi(x, y) = \psi_0 e^{iq_y y}$. Substituting this into Eq. (14), we find that $T - T_c$ has a maximum for $q_y = -\alpha$. Subsequently, we use $\psi(x, y) = \psi(x)e^{-i\alpha y}$, apply separation of variables to Eq. (14), and evaluate the derivatives with respect to y separately. These can be considered as a constant offset to T_c that results in local modulations in T_c. In the presence of SOC, T_c increases according to

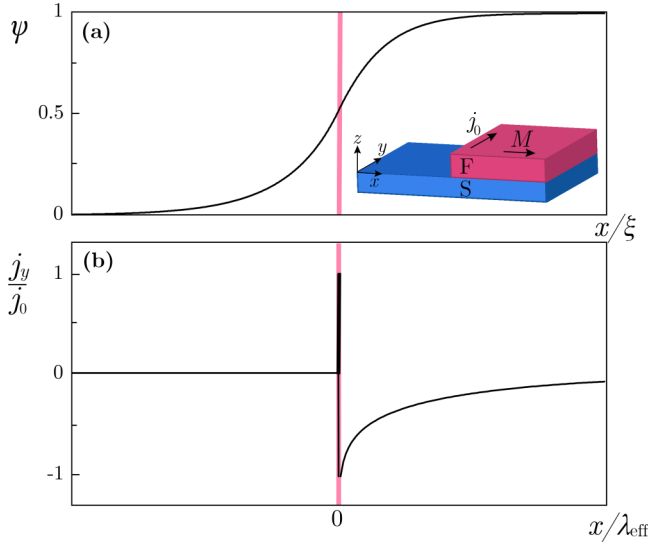$$T_{c+} = T_c\left(1 + \frac{\alpha^2}{4ma_0}\right). \quad (16)$$

FIG. 3. A superconducting film half covered by a ferromagnetic metal with $T \lesssim T_c$. Inset: A schematic illustration of S/F heterostructure with magnetization $\vec{M}$ and edge current $j_0 \hat{y}$. Spatial dependence of (a) the normalized wave function $\psi(x)$ and (b) the current density $j_y(x)$.

We note that T_c in Eq. (16) relates to the critical temperature of the F/S bilayer without SOC, meaning that $T_{c+} - T_c$ represents a recovery of the critical temperature.

We use the modulated critical temperature (16) to consider an F covering the half space [i.e., $x \in [0, \infty)$; see Fig. 3(a)], with $T \lesssim T_c$. We use Eq. (16) to solve Eq. (14).

The total current consists of a current along the edge and the supercurrent, i.e.,

$$\vec{j}(x) = j_0 \delta(x)\hat{y} - \frac{1}{4\pi \lambda_{\text{eff}}} \vec{A}(x). \quad (17)$$

Modeling the edge current as a Dirac δ function is validated by $\xi \ll \lambda$ (London theory). We use Biot-Savart's law $\vec{A} = \int \vec{j}/\sqrt{x^2 + y^2} \, d\vec{l}$, which results in an implicit equation for $\vec{A}$. To avoid divergence issues, we integrate over a strip of width L and set $z = 0$ and obtain

$$A_y(x) = \ln|x - L| - \ln|x|$$
$$+ \frac{1}{2\pi} \int_0^L A_y(x') \ln|x - x'| dx'. \quad (18)$$

We solve the above for $A_y(x)$ iteratively, letting $L \to \infty$ and obtain the current density from Eq. (17). The normalized wave function $\psi(x)$ and current density $j_y(x)$ from Eq. (17) are displayed in Fig. 3. The amplitude of the wave function increases near the edge and saturates inside F. The current is zero outside F and has a δ peak resulting from the edge current, then drops and gradually recovers inside F.

In summary, we have theoretically investigated the role of SOC in S/F junctions in the superconducting state. Firstly, we show that even weak SOC ($\alpha \simeq 0.01/\xi$) lowers the critical field h_{c1}, enabling spontaneous generation of vortex-antivortex pairs. Furthermore, the interaction between vortices and SOC is attractive and so pins vortices along the F edges. Secondly, the suppressed T_c of the F/S bilayer is partially recovered in the presence of SOC and thirdly, the superconducting order parameter ψ is spatially modulated due to SOC in conjunction with a magnetic exchange field. Spontaneous vortex generation and pinning would manifest experimentally as a peak in magnetic field profile in the superconducting layer across the ferromagnet strip's edge below T_c. By measuring local magnetic fields through T_c it would be possible to distinguish the effect of SOC from stray fields from out-of-plane domain walls. Vortex generation and pinning are prominent when the magnetization is perpendicular to the ferromagnet strip's edge and diminish as the magnetization rotates in-plane to vanish when the magnetization is parallel to the ferromagnet strip's edge. Although our model considers a F metal with intrinsic SOC, matching behavior is expected by introducing an interface material with strong SOC [58] such as Pt or Pd, which have high interfacial transparency with Nb [59,60]. An important aspect of our theory is that it raises the prospect for vortex guiding without the usual requirement of stray magnetic fields to generate vortex-antivortex pairs and that vortex motion [see Figs. 1(a) and 1(b)] is reversible with current or magnetization direction. These are key requirements for Abrikosov memory.

[1] A. I. Buzdin, Rev. Mod. Phys. **77**, 935 (2005).

[2] C. Kittel, *Introduction to Solid State Physics* (Wiley, New York, 1996), Chap. 12.

[3] J. W. A. Robinson, S. Piano, G. Burnell, C. Bell, and M. G. Blamire, Phys. Rev. Lett. **97**, 177003 (2006).

[4] J. W. A. Robinson, S. Piano, G. Burnell, C. Bell, and M. G. Blamire, Phys. Rev. B **76**, 094522 (2007).

[5] J. W. A. Robinson, S. Piano, G. Burnell, C. Bell, and M. G. Blamire, IEEE Trans. Appl. Supercond. **17**, 641 (2007).

[6] S. Piano, J. W. Robinson, G. Burnell, and M. G. Blamire, Eur. Phys. J. B **58**, 123 (2007).

[7] Z. Radović, M. Ledvij, L. Dobrosavljević-Grujić, A. I. Buzdin, and J. R. Clem, Phys. Rev. B **44**, 759 (1991).

[8] L. Bulaevskii, V. Kuzii, and A. Sobyanin, Pis'ma Zh. Eksp. Teor. Fiz. **25**, 314 (1977) [JETP Lett. **25**, 290 (1977)].

[9] A. Buzdin, L. Bulaevskii, and S. Panyukov, Pis'ma Zh. Eksp. Teor. Fiz. **35**, 147 (1982) [JETP Lett. **35**, 178 (1982)].

[10] A. Buzdin and M. Kupriyanov, Pis'ma Zh. Eksp. Teor. Fiz. **53**, 308 (1991) [JETP Lett. **53**, 321 (1991)].

[11] J. Y. Gu, C.-Y. You, J. S. Jiang, J. Pearson, Y. B. Bazaliy, and S. D. Bader, Phys. Rev. Lett. **89**, 267001 (2002).

[12] N. Banerjee, C. Smiet, R. Smits, A. Ozaeta, F. Bergeret, M. Blamire, and J. Robinson, Nat. Commun. **5**, 3048 (2014).

[13] P. D. Gennes, Phys. Lett. **23**, 10 (1966).

[14] L. R. Tagirov, Phys. Rev. Lett. **83**, 2058 (1999).

[15] A. I. Buzdin, A. V. Vedyayev, and N. V. Ryzhanova, Europhys. Lett. **48**, 686 (1999).

[16] X. L. Wang, A. Di Bernardo, N. Banerjee, A. Wells, F. S. Bergeret, M. G. Blamire, and J. W. A. Robinson, Phys. Rev. B **89**, 140508(R) (2014).

[17] Z. Feng, J. W. A. Robinson, and M. G. Blamire, Appl. Phys. Lett. **111**, 042602 (2017).

[18] A. Srivastava, L. A. B. Olde Olthof, A. Di Bernardo, S. Komori, M. Amado, C. Palomares-Garcia, M. Alidoust, K. Halterman, M. G. Blamire, and J. W. A. Robinson, Phys. Rev. Appl. **8**, 044008 (2017).

[19] L. G. Johnsen, N. Banerjee, and J. Linder, Phys. Rev. B **99**, 134516 (2019).

[20] C. Bell, G. Burnell, C. W. Leung, E. J. Tarte, D.-J. Kang, and M. G. Blamire, Appl. Phys. Lett. **84**, 1153 (2004).

[21] B. M. Niedzielski, T. J. Bertus, J. A. Glick, R. Loloee, W. P. Pratt, and N. O. Birge, Phys. Rev. B **97**, 024517 (2018).

[22] A. V. Samokhvalov, J. W. A. Robinson, and A. I. Buzdin, Phys. Rev. B **100**, 014509 (2019).

[23] F. S. Bergeret and I. V. Tokatly, Phys. Rev. Lett. **110**, 117003 (2013).

[24] F. S. Bergeret and I. V. Tokatly, Phys. Rev. B **89**, 134517 (2014).

[25] I. V. Bobkova, A. M. Bobkov, and M. A. Silaev, Phys. Rev. B **96**, 094506 (2017).

[26] R. Keizer, S. Goennenwein, T. Klapwijk, G. Miao, G. Xiao, and A. Gupta, Nature (London) **439**, 825 (2006).

[27] M. S. Anwar, F. Czeschka, M. Hesselberth, M. Porcu, and J. Aarts, Phys. Rev. B **82**, 100501(R) (2010).

[28] T. S. Khaire, M. A. Khasawneh, W. P. Pratt, and N. O. Birge, Phys. Rev. Lett. **104**, 137002 (2010).

[29] J. W. A. Robinson, J. D. S. Witt, and M. G. Blamire, Science **329**, 59 (2010).

[30] J. Robinson, F. Chiodi, M. Egilmez, B. Gábor, and M. Blamire, Sci. Rep. **2**, 699 (2012).

[31] J. W. A. Robinson, N. Banerjee, and M. G. Blamire, Phys. Rev. B **89**, 104505 (2014).

[32] N. Banerjee, J. Robinson, and M. Blamire, Nat. Commun. **5**, 4771 (2014).

[33] J. Linder and J. Robinson, Nat. Phys. **11**, 307 (2015).

[34] V. M. Edelstein, Phys. Rev. B **67**, 020505(R) (2003).

[35] A. Buzdin, Phys. Rev. Lett. **101**, 107005 (2008).

[36] S. V. Mironov, A. S. Mel'nikov, and A. I. Buzdin, Phys. Rev. Lett. **114**, 227001 (2015).

[37] S. H. Jacobsen, I. Kulagina, and J. Linder, Sci. Rep. **6**, 23926 (2016).

[38] S. Takada, Progr. Theor. Phys. **43**, 27 (1970).

[39] L. P. Gor'kov and E. I. Rashba, Phys. Rev. Lett. **87**, 037004 (2001).

[40] X. Montiel and M. Eschrig, Phys. Rev. B **98**, 104513 (2018).

[41] K.-R. Jeon, C. Ciccarelli, H. Kurebayashi, L. F. Cohen, X. Montiel, M. Eschrig, S. Komori, J. W. A. Robinson, and M. G. Blamire, Phys. Rev. B **99**, 024507 (2019).

[42] K.-R. Jeon, C. Ciccarelli, A. J. Ferguson, H. Kurebayashi, L. F. Cohen, X. Montiel, M. Eschrig, J. W. Robinson, and M. G. Blamire, Nat. Mater. **17**, 499 (2018).

[43] S. Mironov and A. Buzdin, Phys. Rev. Lett. **118**, 077001 (2017).

[44] S. S. Pershoguba, K. Björnson, A. M. Black-Schaffer, and A. V. Balatsky, Phys. Rev. Lett. **115**, 116602 (2015).

[45] A. G. Mal'shukov, Phys. Rev. B **93**, 054511 (2016).

[46] J. W. A. Robinson, A. V. Samokhvalov, and A. I. Buzdin, Phys. Rev. B **99**, 180501(R) (2019).

[47] J. Baumard, J. Cayssol, F. S. Bergeret, and A. Buzdin, Phys. Rev. B **99**, 014511 (2019).

[48] O. Dimitrova and M. V. Feigel'man, Phys. Rev. B **76**, 014522 (2007).

[49] V. M. Edelstein, J. Phys.: Condens. Matter **8**, 339 (1996).

[50] V. Mineev and M. Sigrist, *Basic Theory of Superconductivity in Metals Without Inversion Center* (Springer, New York, 2012).

[51] See Supplemental Material at http://link.aps.org/supplemental/10.1103/PhysRevB.100.220505 for detailed derivations of the equations in the main text.

[52] P. De Gennes, *Superconductivity of Metals and Alloys*, Advanced Book Classics (Westview Press, Boulder, CO, 1966).

[53] If we consider Eq. (6) in the absence of vorticity ($\Phi_q = 0$), the remaining term is the anomalous phase $\varphi = \vec{\alpha} \cdot \vec{r}$. This shows the equivalence between an S with a phase and an S with a vector potential.

[54] The sign of the magnetic field spikes in Fig. 1(d) corresponds to the magnetization direction $\hat{x}$. Reversing it to $-\hat{x}$ flips the sign of the spikes.

[55] V. K. Vlasko-Vlasov, F. Colauto, A. I. Buzdin, D. Rosenmann, T. Benseman, and W.-K. Kwok, Phys. Rev. B **95**, 144504 (2017).

[56] Y. M. Shukrinov, A. Mazanik, I. R. Rahmonov, A. E. Botha, and A. Buzdin, Europhys. Lett. **122**, 37001 (2018).

[57] A. Manchon, H. C. Koo, J. Nitta, S. M. Frolov, and R. A. Duine, Nat. Mater. **14**, 871 (2015).

[58] S. H. Jacobsen, J. A. Ouassou, and J. Linder, Phys. Rev. B **92**, 024510 (2015).

[59] X. Tao, Q. Liu, B. Miao, R. Yu, Z. Feng, L. Sun, B. You, J. Du, K. Chen, S. Zhang, L. Zhang, Z. Yuan, D. Wu, and H. Ding, Sci. Adv. **4**, eaat1670 (2018).

[60] A. Ghosh, K. Garello, C. O. Avci, M. Gabureac, and P. Gambardella, Phys. Rev. Appl. **7**, 014004 (2017).